STUDY OF VARIATION IN POROSITY AND ITS ASSOCIATED PARAMETERS DUE TO CU DOPING IN ZINC FERRITE USING SOL-GEL AUTO-COMBUSTION METHOD

Shrinivas JAMDADE[1], Popat TAMBADE[2], Sopan RATHOD[3]

In this study, the effect of compositional variation on porosity along with change in structure and magnetic parameters associated with porosity were reported owing to the doping of Cu in zinc ferrite. Cu doped zinc ferrites having chemical formula $Cu_xZn_{1-x}Fe_2O_4$ (x = 0.1, 0.2, 0.3, 0.4, 0.5, 0.6 and 0.7) were prepared by Sol-Gel auto combustion method. We found porosity decreases with increase in Cu concentration. Analysis shows that structural parameters, dislocation density, and lattice strain decreases non-monotonically while magnetic parameters, initial permeability, and anisotropic constant decreases non-linearly with increase in porosity of samples.

Keywords: Sol-Gel Auto-combustion Method, Cu doping in Zinc Ferrite, Porosity

1. Introduction

CuZn ferrite is a soft magnetic material that is a part of spinel family. $ZnFe_2O_4$ is usually assumed to be a normal spinel with all eight Zn^{2+} ions on A site and all eight Fe^{3+} ions on B site. The doping of Cu^{2+} in place of Zn^{2+} changes the cation distribution and magnetic ordering in the spinel structure. There by structural and magnetic properties are changed. CuZn ferrite offer superior magnetic properties depending on concentration of Cu and Zn in the ferrite [1-4].

For different applications many synthesis methods like ceramic, co-precipitation, hydro-thermal, solvo-thermal, sono-chemical, Sol-Gel, micro-emulsion, aerosol, etc. are used. The sol-gel auto-combustion method is simple, rapid, convenient, efficient, low cost, ecofriendly at low temperature [5-9].

The sintering process does not produce an entirely dense material but samples having a certain porosity. The porosity of ferrite is the relative volume of pores it contains. The different properties of ferrites can be optimized by changing the process parameters. The two most important properties of magnetic materials are initial permeability and coercivity. Both of these properties are dependent not only on the composition of the ferrite, but also on the microstructure and crystal

[1] Nowrosjee Wadia College, Pune, India, e-mail: hv_jamdade@yahoo.com
[2] Prof. Ramkrishna More Arts, Commerce and Science College, Akurdi, Pune, India, e-mail: pstam3@rediffmail.com
[3] MES Abasaheb Garware College, Pune, India, e-mail: smragc@rediffmail.com

lattice defects in the ferrite. These parameters deteriorate the magnetic character of ferrites [10-15].

This work deals with dependence of initial permeability and coercivity on porosity of the ferrite. The studies objective is to investigate effect of structural property, porosity on magnetic parameters, initial permeability and coercivity as the Cu doping in Zn ferrite is increased. The porosity plays vital role in determining the characteristics of ferrites [16-18].

To our information the porosity of nano size $Cu_xZn_{1-x}Fe_2O_4$ ferrite synthesized by sol-gel auto-combustion method is presented and discussed for the first time in this study.

2. Experimental Procedure

Cu doped zinc ferrites having chemical formula $Cu_xZn_{1-x}Fe_2O_4$ (x = 0.1, 0.2, 0.3, 0.4, 0.5, 0.6 and 0.7) were prepared by Sol-Gel auto-combustion method. In the present work, copper nitrate trihydrate ($(Cu(NO_3)_2).3H_2O$), zinc nitrate hexahydrate ($(Zn(NO_3)_2).6H_2O$), ferric nitrate nonahydrate ($(Fe(NO_3)_2).9H_2O$) was used. The proportion of nitrates to citrate was kept at 1:3. Mixed solution was heated at 80° C for one hour to get a gel. The gel was burned to get the ferrite in the form of ash. This ash residue was grounded in agate mortar to get homogenous powder. The sintering was carried at 400° C for 4 hours and used for further characterizations. This way, $Cu_xZn_{1-x}Fe_2O_4$ ferrite samples were prepared with x = 0.1, 0.2, 0.3, 0.4, 0.5, 0.6, and 0.7 [19-21].

Bulk density (D_{bulk}), Theoretical density or X-ray density (D_{Xray}), and porosity (ρ) of the sintered samples are calculated by using well known formulas given below.

$$D_{Bulk} = \frac{m}{\pi \times r^2 \times h} \tag{1}$$

$$D_{Xray} = \frac{8M}{N_A V} \qquad 8 \text{ for Cubic} \tag{2}$$

$$\text{Porosity} = \frac{D_{Xray} - D_{Bulk}}{D_{Xray}} \times 100 \tag{3}$$

Where m is mass, r is radius, h is sample / pellet thickness / height, M is molecular weight, N_A is Avogadro number, V is cell volume, D_{Bulk} is bulk density, D_{Xray} is x-ray density.

The initial permeability is mainly due to the rotation and displacement process of domain structure. Grain size (D), saturation magnetization (M_S), and initial permeability (μ_i) are interlinked by the following relation

$$\mu_i = \frac{M_S{}^2 D}{K_1} = \mu_{iRotation} + \mu_{iDisplacement} \quad (4)$$

Where K_1 is anisotropic constant.

In the case of ferrite whose porosity is too great and whose pores are finely distributed, the rotation process of domain wall movement makes contribution to μ_i. The initial permeability of rotation process depends on anisotropic forces and if magnetic anisotropy prevails then

$$\mu_{iRotation} = \left(\frac{2\pi M_S{}^2}{K_1} \right) + 1 \quad (5)$$

Coercivity (Hc) is generally governed by the magneto crystalline anisotropy constant (K_1), permeability (μ_0), and saturation magnetization (M_S) through the Brown relationship which is given as

$$H_C = \frac{2K_1}{\mu_0 M_S} \quad (6)$$

In ferro-spinel's due to the cubic symmetry of the crystal structure and very low coercive force, the magnetization by rotation process predominates as single domain magnetic structure in the grains are seen [22-25].

In this study, crystallite size, lattice strain, dislocation density, and lattice parameter are calculated from XRD data while grain size is calculated from FESEM micrograph. The saturation magnetization (M_S), initial permeability (μ_i), Coercivity (H_C), and anisotropy constant (K_1) are calculated from the VSM analysis [26-29].

3. Results and Discussions

Fig. 1 shows variation in porosity, initial permeability, coercivity with respect to Cu concentration and coercivity vs porosity. The results obtained are mentioned in the table 1. The crystallite size varies from 5.92 to 7.69 nm for x composition of Cu doping. The anisotropy constant changes from 2.20 to 6.49 while initial permeability varies from 344.17 to 1275.35. The results showed that the lattice strain (ε) decreased showing variation from 0.142 to 0.117 for x different composition of Cu doping.

The ferrite specimens under study are found to be porous with the average porosity lied ~ 49%. The porosity of nanomaterials determines the stability of the initially nucleated particles. We found porosity decreases with the increase in Cu concentration. This decrease in porosity is seen up to x = 0.5 composition and thereafter it shows non-monotonic increase with Cu doping which can be correlated with the inter-granular defects and defects of an interface between grain boundaries. The increase in initial permeability with composition is related to increased crystallite size and magnetic anisotropy.

The coercivity non-monotonically increases with Cu doping. We observe coercivity being maximum for x = 0.5. In pores samples fewer domain walls are present thereby a very slow increase in coercivity is seen.

Table 1

Diffraction Angle (2θ), Lattice Parameter (a), Volume of Cell (Vcell), X-ray Density (DX), Crystallite Size (D), Strain (ε), Dislocation Density (δ), Coercivity (H_C), Saturation Magnetization (M_S), Molecular Weight of Composition, and Anisotropic Constant (K) with substitution for $Cu_xZn_{1-x}Fe_2O_4$.

x	0.1	0.2	0.3	0.4	0.5	0.6	0.7
2θ	35.2	35.36	35.2	35.4	35.36	35.62	35.52
Lattice Parameter (a) Å	8.45	8.41	8.45	8.4	8.4	8.35	8.37
Vcell ($Å^3$)	603.07	595.17	603.06	593.22	595.17	582.65	587.42
X-ray Density (DX) (g/cc)	5.337	5.403	5.328	5.413	5.391	5.503	5.454
D (nm) (D-S Method)	6.44	6.18	5.92	6.79	6.66	6.5	7.69
Strain (ε) (D-S Method)	0.142	0.146	0.153	0.133	0.136	0.139	0.117
Dislocation Density (δ) (g/cc)	0.027	0.029	0.023	0.023	0.024	0.017	0.027
H_C (Oe)	0.195	0.151	0.145	0.191	0.201	0.175	0.191
M_S (emu/g)	10.848	18.496	20.592	24.304	28.688	26.688	32.801
Molecular Weight of Composition (g)	242.267	242.083	241.899	241.716	241.533	241.345	241.166
Anisotropic Constant	2.2	2.89	3.11	4.81	5.97	4.86	6.49

Fig. 2 shows graphs of initial permeability, dislocation density, anisotropy constant, lattice strain, crystallite size, and lattice parameter with respect to porosity. Analysis shows that lattice parameter, and crystallite size increases non-monotonically with porosity. The rate of increase is measured by measuring the slope of the fitted broken line model. The rate of increase is 0.16 %, and 1.8 % respectively. We also found that dislocation density, anisotropy constant, and lattice strain decrease non-linearly with increase in porosity of samples. The rate of decrease in initial permeability is largest as compared to the other parameters in $Cu_xZn_{1-x}Fe_2O_4$ ferrite.

This trend can be interpreted by the fact that doping of small amounts of Cu ions stimulates nucleation, and growth process which tends to the appreciation of nano crystallites whose size steadily increase with doping percentage due to the bigger radius of Cu than that of Zn. For higher Cu density, the decrease of lattice strain (ε) can be associated with low solubility of Cu ions into the Zn lattice.

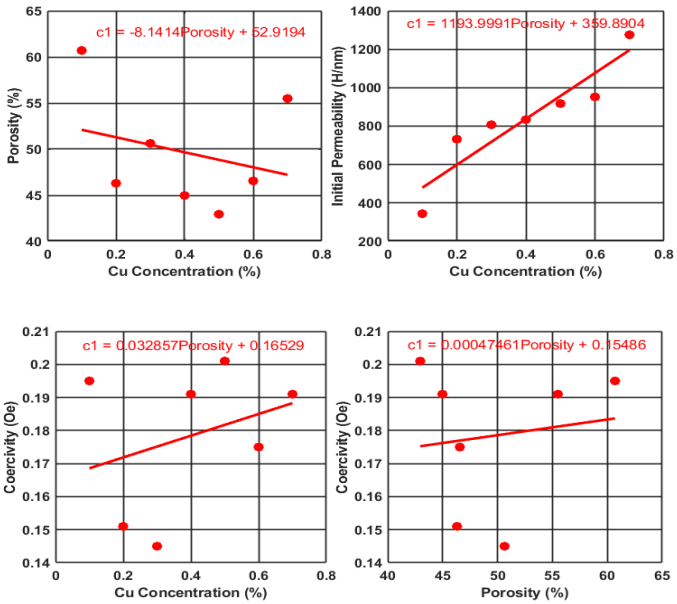

Fig. 1. Variation in Porosity, Initial Permeability, Coercivity with respect to Cu Concentration and Coercivity vs Porosity.

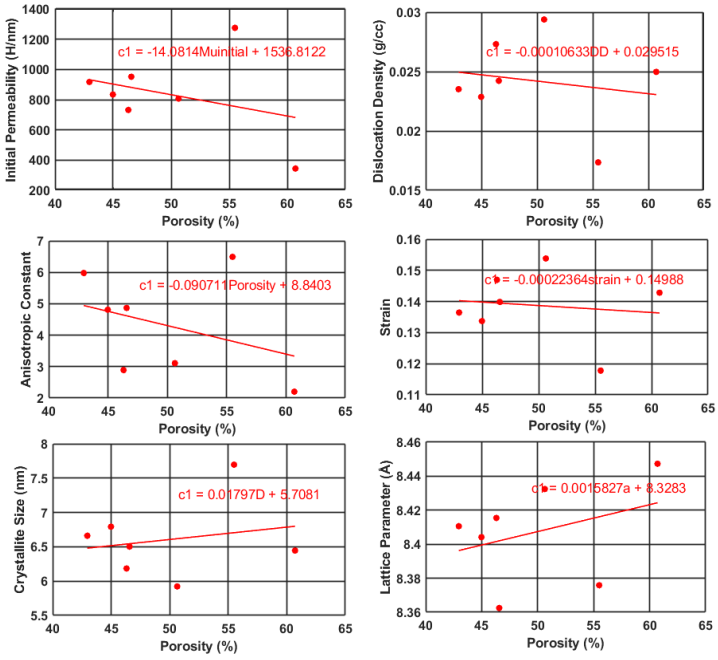

Fig. 2. Variation in Initial Permeability, Dislocation Density, Anisotropic Constant, Strain, Crystallite Size, and Lattice Parameter with respect to Porosity

4. Conclusions

Magnetization of ultra-soft magnetic ferrite is determined by the rotation process of domains. The movement of rotation can be hampered by porosity. The decrease in porosity results in an increase of initial permeability. With slight slow increase in crystallite size from 5.92 to 7.69 nm, initial permeability increase from 344.17 to 1275.35 H/nm is observed. Low coercivity is obtained when the crystallites have sufficiently small size and samples have large porosity up to 50%. When the rotation process of magnetization prevails, one has a single domain magnetic structure in grain which results in lowering coercivity of ferrite material making it an ultrasoft magnet. This way porosity changes values of initial permeability and coercivity of samples.

REFERENCES

[1] *S.M. Rathod, A.R. Chavan, S.S. Jadhav, K.M. Batoo, M. Hadi, and E.H. Raslan*, Ag^{+} ion substituted $CuFe_2O_4$ nanoparticles: Analysis of structural and magnetic behavior, Chemical Physics Letters, **vol. 765**, 2021, pp. 138308.

[2] *S. M. Rathod, V.G. Deonikar, and P.P. Mirage*, Synthesis of Nano-Sized Cerium Doped Copper Ferrite, Their Magnetic and Optical Studies, Journal of Computational and Theoretical Nanoscience, **vol. 22**, 2016, pp. 964-966.

[3] *A. Nihore, F. Aziz, N. Oswal, P. Jain, O. Subohi, and N. Gupta*, Synthesis and characterization of copper doped nickel ferrite prepared by Sol-gel Method, Materials Today: Proceedings, **vol. 18(7)**, 2019, pp. 3651-3656.

[4] *A.A. Khan, S.N. Khan, and A. Mir*, Structural and electromagnetic characterization of yttrium doped copper ferrite, Journal of Magnetism and Magnetic Materials, **vol. 559(7)**, 2022, pp. 169510.

[5] *R. Dhyani, R.C. Srivastava, P.S. Rawat, and G. Dixit*, Structural and elastic properties of tetragonal nano-structured copper ferrite, International Journal of Materials Research, **vol. 113(10)**, 2022, pp. 9.

[6] *R. Khunphonoi, P. Khemthong, C. Luadthong, and K. Faungnawakij*, Correlating the effect of preparation methods on the structural and magnetic properties, and reducibility of $CuFe_2O_4$ catalysts, RSC Advances, **vol. 12(24)**, 2022, pp. 15526-15533.

[7] *K.R. Sanadi, S.P. Patil, and V.B. Helavi*, Structural and electrical properties of cobalt substituted copper ferrites synthesized by Sol-Gel auto-combustion method, Materials Focus, **vol. 6**, 2017, pp. 1-6.

[8] *G. Thirupathi, and R. Singh*, Magnetic properties of zinc ferrite nanoparticles, IEEE Transactions on Magnetics, **vol. 48(11)**, 2021, pp. 3630-3633.

[9] *A. Saleem, Y. Zhang, H. Gong, M.K. Majeed, X. Lin, M.M. Hussain, and M.Z. Ashfaq*, Electromagnetic wave absorption performance of Ni doped Cu-ferrite nanocrystals, Materials Research Express, **vol. 7**, 2020, pp. 016117.

[10] *S. Bhaskarana, I.A. Al-Omarib, and E.V. Gopalan*, On the enhanced coercive field and anisotropy observed in cobalt substituted copper ferrite nanoparticles prepared by a modified sol-gel method, Journal of Alloys and Compounds, **vol. 884**, 2021, pp. 161095.

[11] *A. Subha, M.G. Shalini, B. Sahu, and S.C. Sahoo*, Structural transformation and magnetic properties of copper ferrite nanoparticles prepared by sol-gel method, Journal of Materials Science: Materials in Electronics, **vol. 29**, 2018, pp. 20790-20799.

[12] *A. Hakeem, T. Alshahrani, G. Muhammad, M. H. Alhossainy, A. R. Khan, I. Ali, H. M. T. Farid, T. Ghrib, S. R. Ejaz, and R. Y. Khosa*, "Magnetic, dielectric and structural properties of spinel ferrites synthesized by sol-gel method", Journal of Materials Research and Technology, **vol. 11**, 2021, pp. 158-169.

[13] *K. Elayakumar, A. Manikandan, A. Dinesh, K. Thanrasu, K.K. Raja, R.T. Kumar, Y. Slimani, S.K. Jaganathan, and A. Baykal,* "Enhanced magnetic property and antibacterial biomedical activity of Ce^{3+} doped $CuFe_2O_4$ spinel nanoparticles synthesized by sol-gel method", Journal of Magnetism and Magnetic Materials, **vol. 478**, 2019, pp. 140147.

[14] *M.N. Akhtar, M. Babar, S. Qamar, Z.U. Rehman, and M.A. Khan,* "Structural rietveld refinement and magnetic features of prosademium (Pr) doped Cu nanocrystalline spinel ferrites", Ceramics International, **vol. 45(8)**, 2019, pp. 10187-10195.

[15] *T. Roman, A. Pui, A.V. Lukacs, N. Cimpoesu, S. Lupescu, A.I. Borhan, K. Kordatos, A. Ntziouni, P. Postolache, M. Zaharia, S. Stanciu, and L. Mitoseiru,* "Structural changes of cerium doped copper ferrites during sintering process and magneto-electrical properties assessment", Ceramics International, **vol. 45(14)**, 2019, pp. 17243-17251

[16] *R.R. Kanna, K. Sakthipandi, S.M. Seeni, M.A. Maraikkar, N. Lenin, and M. Sivabharathy,* "Doping effect of rare-earth (lanthanum, neodymium and gadolinium) ions on the structural, optical, dielectric and magnetic properties of copper nanoferrites", Journal of Rare Earths, **vol. 36(12)**, 2018, pp. 1299-1309.

[17] *M. Mustaqeem, K. Mahmood, T.A. Saleh, A.U. Rehman, M. Ahmad, Z.A. Gilani, and M. Asif,* "Synthesis of $CuFe_{2-x}Er_xO4$ nanoparticles and their magnetic, structural and dielectric properties", Physica B: Physics of Condensed Matterials, **vol. 588**, 2020, pp. 412176.

[18] *V. Manikandan, V. Kuncser, B. Vasile, S. Kavita, S. Vigneselvan, and R. S. Mane,* "Enhancement in magnetic and dielectric properties of the ruthenium-doped copper ferrite (Ru-$CuFe_2O_4$) nanoparticles", Journal of Magnetism and Magnetic Materials, **vol. 476**, 2019, pp. 18-23.

[19] *R.P. Sharma, S.D. Raut, R.M. Mulani, A.S. Kadam, and R.S. Mane,* "Sol-gel auto-combustion mediated cobalt ferrite nanoparticles: a potential material for antimicrobial applications", International Nano Letters, **vol. 9**, 2019, pp. 141-147.

[20] *J.Y. Hu, X.S. Liu, X.C. Kan, S.J. Feng, C.C. Liu, W. Wang, K.M.U. Rehman, M. Shazed, S.Q. Zhou, and Q.Y. Wu, "*Characterization of texture and magnetic properties of $Ni_{0.5}Zn_{0.5}Ti_xFe_{2-x}O_4$ spinel ferrites", Journal of Magnetism and Magnetic Materials, **vol. 489**, 2019, pp. 165411.

[21] *M.K. Kokare, N.A. Jadhav, V. Singh, and S.M. Rathod, "*Effect of Sm^{3+} substitution on the structural and magnetic properties of NiCo nanoferrites", Optics and Laser Technology, **vol. 112**, 2019, pp. 107-116.

[22] *Y. Gao, Z. Wang, J.J. Pei, and H.M. Zhang, "*Structure and magnetic properties correlated with cation distribution of $Ni_{0.5-x}Mo_xZn_{0.5}Fe_2O_4$ ferrites prepared by sol-gel auto-combustion method", Ceramic International, **vol. 44**, 2018, pp. 20148-20153.

[23] *A. Rękorajska, G. Cichowicz, M.K. Cyranski, M. Grden, M. Pekala, G.J. Blanchard, and P. Krysinski, "*Synthesis and Characterization of Tb-Doped Nanoferrites", Chem Nano Material, **vol. 4**, 2018, pp. 231-242.

[24] *A.U. Rehman, N.A. Morley, N. Amin, M.I. Arshad, M.A. Nabi, K. Mahmood, and F. Iqbal, "*Controllable synthesis of La3+ doped $Zn_{0.5}Co_{0.25}Cu_{0.25}Fe_{2-x}La_xO_4$ (x= 0.0, 0.0125, 0.025, 0.0375, 0.05) nano-ferrites by sol-gel auto-combustion route", Ceramic International, **vol. 46(18(A))**, 2020, pp. 29297-29308.

[25] *V. Awati, K. Badave, and D. Bobade, "*Effect of Tb^{3+} substitution on structural, optical and magnetic properties of $NiCuZnFe_2O_4$ prepared by sol-gel route", Indian Journal of Physics, **vol. 6(1)**, 2022, pp. 89-101.

[26] *K. Hussain, N. Amin, and M.I. Arshad, "*Evaluation of structural, optical, dielectric, electrical, and magnetic properties of Ce^{3+} doped $Cu_{0.5}Cd_{0.25}Co_{0.25}Fe_{2-x}O_4$ spinel nano-ferrites", Ceramic International, **vol. 47**, 2021, pp. 3401-3410.

[27] *K.V. Kumar, "*Tunable optical bandgap of gadolinium substituted nickel-zinc ferrite nanoparticles-effect of calcination temperature on its optical parameters", Advances in Materials Physics and Chemistry, **vol. 12**, 2022, pp. 33-45.

[28] *Y. Slimani, M.A. Almessiere, S. Güner, U. Kurtan, S.E. Shirsath, A. Baykal, and I. Ercan, "*Magnetic and microstructural features of Dy3+ substituted $NiFe_2O_4$ nanoparticles derived by sol-gel approach", Journal of Sol-Gel Science and Technology, **vol. 95(1)**, 2020, pp. 202-210.

[29] *H.F. Devi, K. Thoithoi Devi, and T.D. Singh, "*Synthesis, characterization, optical and electrical properties of citrate mediated terbium doped ZnO nanoparticles for multifunctional applications", Integrated Ferroelectrics, **vol. 204**, 2020, pp. 81-89.